Journal of Plant Physiology 176 (2015) 118–128

Contents lists available at ScienceDirect

Journal of Plant Physiology

journal homepage: www.elsevier.com/locate/jplph

Molecular Biology

Tubulin marker line of grapevine suspension cells as a tool to follow early stress responses

Xin Guan[a,*,1,2], Günther Buchholz[b], Peter Nick[a]

[a] Molecular Cell Biology, Botanical Institute, Karlsruhe Institute of Technology, Kaiserstraße 2, D-76128 Karlsruhe, Germany
[b] RLP AgroScience/AlPlanta – Institute for Plant Research, Breitenweg 71, D-67435 Neustadt an der Weinstraße, Germany

ARTICLE INFO

Article history:
Received 16 June 2014
Received in revised form 29 October 2014
Accepted 31 October 2014
Available online 22 December 2014

Keywords:
Auxin
Green fluorescent protein (GFP)
Grapevine, transgenic
Microtubule
Vitis rupestris

ABSTRACT

Plant microtubules (MTs), in addition to their role in cell division and cell expansion, respond to various stress signals. To understand the biological function of this early response requires non-destructive strategies for visualization in cellular models that are highly responsive to stress signals. We have therefore generated a transgenic tubulin marker line for a cell line from the grapevine *Vitis rupestris* that readily responds to stress factors of defense-related and abiotic stresses based on a fusion of the green fluorescent protein with *Arabidopsis* β-tubulin 6. By a combination of spinning-disk confocal microscopy with quantitative image analysis, we could detect early and specific responses of MTs to defense-related and abiotic stress factors *in vivo*. We observed that Harpin Z (HrpZ), a bacterial elicitor that can trigger programmed cell death, rapidly eliminated radial MTs, followed by a slower depletion of the cortical array. Jasmonic acid (JA), in contrast, induced bundling of cortical MTs. Auxin reduced the thickness of cortical MTs. This effect followed a characteristic bell-shaped dose-dependency and could revert JA-induced bundling. Impeded cell expansion as a consequence of stress treatment or superoptimal auxin was linked with the appearance of intranuclear tubulin speckles. The early and stimulus-specific responses of MTs are discussed with respect to a function in processing or decoding of stress signals.

Introduction

Similar to their animal counterparts, plant microtubules (MTs) are pivotal for cell division. In addition, the cortical array of MTs controls the spatial organization of cell expansion. It was this plant-specific function that half a century ago led first to the prediction (Green, 1962), and finally to the discovery (Ledbetter and Porter, 1963) of MTs. Although MTs are fairly conservative in molecular terms, their role in cell expansion is not the only issue specific for plants. During recent years, a novel function of MTs in the sensing and processing of stimuli has emerged (for review, see Nick, 2013). Due to their nonlinear dynamic (Sataric and Tuszynski, 2005) assembly and catastrophic disassembly, MTs can act as amplifiers of signals and also decode temporal patterns such as stress signatures.

As expected from a role in signal processing, evidence for a sensory role of MTs has accumulated, such as perception of mechanical strain patterns during phyllotaxis (Hardham et al., 1980; Hamant et al., 2008), or gravitropism (Nick et al., 1991; Godbolé et al., 2000), perception of low temperature (Abdrakhamanova et al., 2003), or the sensing of osmotic challenge (Komis et al., 2002; Wang et al., 2011; Liu et al., 2013).

If MTs are endowed with a sensory role, they should be highly responsive to the inducing stimulus and this response should precede other responses such as gene activation. Signal-triggered MT responses have been discovered by immunofluorescence for situations where these responses have spread to the majority of the cytoskeleton, and this has allowed an understanding of the role of MT reorientation contributing to signal-dependent growth responses based on comparative time-course studies (for review, see Nick, 1999). However, the more subtle early responses relevant for the sensory functions of MTs cannot be addressed by this approach, because the variability between individual cells of a tissue or a cell population in a suspension culture with respect to MT organization exceed by far the early, rapid and more delicate changes induced by a stimulus. To detect such early changes, MTs must be followed in a given cell over time. This approach requires a non-destructive method of visualization. Fluorescently tagged cytoskeletal marker lines have been a valuable tool in this respect.

Abbreviations: ETI, effector-triggered immunity; HrpZ, Harpin Z; IAA, indolyl-3-acetic acid; JA, (±)-jasmonic acid; MTs, microtubules; PCV, packed cell volume; PTI, pathogen-associated molecular pattern (PAMP) triggered immunity.

* Corresponding author.
E-mail address: xinguan.cnde@googlemail.com (X. Guan).
[1] Present address: College of Horticulture and Landscape Architecture, Southwest University, 400716 Chongqing, China.
[2] Present address: Laboratoire Vigne Biotechnologies et Environnement EA-3991, Université de Haute-Alsace, 68000 Colmar, France.

http://dx.doi.org/10.1016/j.jplph.2014.10.023
0176-1617/

A role of MTs has also been proposed for plant defense (for review, see Takemoto and Hardham, 2004; Kobayashi and Kobayashi, 2008), but this was mainly attributed to downstream responses such as papillae formation or cell-wall synthesis. However, recently it was demonstrated that pharmacological manipulation of MTs can activate defense-related gene expression in cell lines of grapevine (Qiao et al., 2010) suggesting that, similar to abiotic stress, biotic interactions can also be sensed through MT-dependent signaling. This gene activation was related to the induction and metabolism of antimicrobial phytoalexins. In a cell line from the wild North American grapevine *Vitis rupestris*, the MT-dependency of gene activation was most pronounced, and the same held true for the induction of the highly bioactive stilbene resveratrol and its potent oxidized dimer δ-viniferin (Chang and Nick, 2012) associated with the induction of defense-related programmed cell death.

In our previous work, we have addressed the responses of the cytoskeleton to flg22, an inducer of basic innate immunity, and the phytobacterial elicitor $HrpZ_{Psph}$, making use of fluorescently tagged marker cell lines that had been generated in tobacco BY-2 (Wei et al., 1992; Guan et al., 2013a). This approach was successful in detecting early responses of submembraneous actin filaments, whereas MTs appeared to respond only to Harpin Z (HrpZ). To understand the function of these cytoskeletal responses in the context of defense, it would be necessary to link them with activation of defense genes and the synthesis of phytoalexins. A drawback of the BY-2 system is that the physiological framework of defense has not been worked out thus far. We therefore decided to return to the *V. rupestris* cell lines. As a precondition, a GFP-tagged tubulin marker line had to be generated in the background of this line.

Vitis transformation is a time-consuming task and, depending on the transgenes or varieties, may even fail completely (Schellenbaum et al., 2008; Guan et al., 2013b). We succeeded in generating a fluorescently tagged actin marker line in grapevine (Guan et al., 2014), and therefore ventured to generate a MT marker line in *V. rupestris* using *Arabidopsis* β-tubulin 6 (At5g12250) in fusion with GFP. Using this novel tool in combination with spinning disk confocal microscopy, we were able to visualize early responses of MTs to different defense-related and abiotic stress signals, to identify signal-specific reorganization events, and to gain insight into the role of the phytohormones jasmonic acid (JA) and auxin in stress-induced microtubular remodeling.

Materials and methods

Plasmid construct

The *Agrobacterium tumefaciens* strain harboring the construct pCambia1300_$(CAA)_n$_2 × T-GFP-AtTUB6 was generated as follows: the region encoding the GFP-AtTUB6 (GFP in fusion with the N-terminus of *Arabidopsis* β-tubulin 6 (At5g12250), Nakamura et al., 2004) was amplified by PCR using the following primers: 5′-TCTAGAATGAGTAAAGGAGAAGAAC-3′ containing a *Xba*I restriction site (underlined), and 5′-GAGCTCTCACTCATGATCCAATATCTC-3′ containing a *Sac*I restriction site (underlined) from pBI121-GFP-AtTUB6 (kind gift of Dr. T. Hashimoto). The insert was then introduced into the binary vector pCambia1300 $(CAA)_n$_2 × T harboring an optimized translation initiation site (De Amicis et al., 2007) and a CaMV35S-nos double-terminator for reduced RDR6-mediated gene silencing (Luo and Chen, 2007). In this construct, GFP-AtTUB6 was under control of the constitutive CaMV-35S promoter. The construct was introduced into the *A. tumefaciens* strain EHA105 using an improved freeze–thaw transformation protocol (Chen et al., 1994): after thawing cells at room temperature for 10 min, 700 ng of plasmid DNA were added to competent cells, and mixed gently. After shock-freezing the cells in liquid nitrogen for 1 min, they were thawed for 5 min at 37 °C in a water bath. 500 μL of LB medium (Bertani, 1951. Duchefa, Haarlem, The Netherlands) were added and incubated shaking at 28 °C for 2 h. Subsequently, cells were spun down briefly, and about 300–400 μL of the supernatant was removed. The pellet in the remaining volume of 100–200 μL was then resuspended and plated on solid LB medium with 30 μg mL^{-1} Hygromycin, 15 μg mL^{-1} Rifampicin, and 300 μg mL^{-1} Streptomycin. Colonies appeared after 2–3 days at 28 °C.

Preparation of suspension cells and Agrobacterium for transformation

Suspension cell cultures of *Vitis rupestris* generated from leaves (Seibicke, 2002) were used in this experiment. They were cultivated in liquid medium containing 4.3 g L^{-1} Murashige and Skoog salts (1962, Duchefa, Haarlem, The Netherlands), 30 g L^{-1} sucrose, 200 mg L^{-1} KH_2PO_4, 100 mg L^{-1} inositol, 1 mg L^{-1} thiamine, and 0.2 mg L^{-1} 2,4-dichlorophenoxyacetic acid (2,4-D), adjusted to a final pH of 5.8. Cells were subcultured weekly, inoculating 10 mL of stationary cells into 30 mL of fresh medium in 100 mL Erlenmeyer flasks. The cell suspensions were incubated at 25 °C in the dark on an orbital shaker (KS250 basic, IKA Labortechnik, Staufen, Germany) at 150 rpm. A single colony of *A. tumefaciens* strain EHA105 was inoculated into 20 mL of LB medium supplemented with the appropriate antibiotics. The bacterial cultures were incubated at 28 °C at 200 rpm on an orbital shaker for 48 h.

Pre-culture and co-cultivation

30 μL *Agrobacterium* (cultivated in LB medium to an optical density at 600 nm of 0.6–2.0) were inoculated into 25 mL infiltration medium [50 mL 20× AB salt solution (20 g L^{-1} NH_4Cl, 6 g L^{-1} $MgSO_4 \cdot 7H_2O$, 3 g L^{-1} KCl, 0.2 g L^{-1} $CaCl_2$, 15 mg L^{-1} $FeSO_4 \cdot 7H_2O$), 2.4 mL 500 mM phosphate solution (60 g L^{-1} K_2HPO_4, 20 g L^{-1} NaH_2PO_4, pH 7.5), 100 mL 20% (w/v) sucrose, 848 mL 2-ethanesulfonic acid (MES) solution (3.9 g L^{-1} MES, pH 5.8) per liter] with the appropriate antibiotics, and cultivated in a 250 mL flask for one day. The next day, the *Agrobacterium* culture was centrifuged at 5500 rpm for 15 min, and re-suspended in 25 mL induction medium [50 mL 20× AB salt solution, 2.4 mL 500 mM phosphate solution, 100 mL 20% (w/v) glucose, 848 mL MES solution per liter] with the appropriate antibiotics in a 250 mL flask. The next day, *Agrobacterium* was again spun down for 15 min at 5500 rpm, and re-suspended in 25 mL suspension-medium [2.2 g L^{-1} NN_{69} medium (Nitsch and Nitsch, 1969. Duchefa, Haarlem, The Netherlands), 20 g L^{-1} maltose, 4.6 g L^{-1} glycerol, 0.5 g L^{-1} MES, adjusted to a pH of 5.8] supplemented with 1 mg L^{-1} 1-naphthoxyacetic acid (NOA), in a 250-mL flask incubating at 28 °C, 200 rpm on an orbital shaker for 2 h.

On the same day, 7 mL packed cell volume (PCV) of *V. rupestris* suspension cells collected at day 3 after subcultivation and suspended with co-cultivation-medium [2.2 g L^{-1} NN_{69} medium, 20 g L^{-1} maltose, 4.6 g L^{-1} glycerol, 0.5 g L^{-1} MES, 2.5 g L^{-1} PVPP, 3 g L^{-1} gelrite, adjusted to a pH of 5.8], supplemented with 100 μM acetosyringone, were transferred onto filter paper, and briefly dried by a mild vacuum for 3–5 s. Together with the filter paper, the cells were transferred into a petri dish on solid co-cultivation-medium, sealed with parafilm, and kept at 22 °C for two days. Then, drops of the *Agrobacterium* suspension were spread on the precultivated *V. rupestris* cells and co-cultivated for additional 3 days at 22 °C in a phytotron (Kälte Kamrath, Germany), under a light regime of 16 h light/8 h darkness using mixed light of Sylvania GRO-LUX F38W/GRO T8 and OSRAM L38W/840 LUMILUX cool white.

Elimination of Agrobacterium and generation of a suspension cell line

After 3 days of co-cultivation, the filter papers carrying the cells were transferred onto selective medium [30 g L^{-1} NN_{69}-medium sucrose, 3 g L^{-1} gelrite, 50 mg L^{-1} kanamycin, and 500 mg L^{-1} carbenicillin, adjusted to a pH of 5.8]. 1 week later, filter papers with adhering cells were transferred onto fresh selective medium. This subcultivation was repeated at intervals of 4 weeks till a stably transformed callus had been established and sufficient material accumulated to launch a suspension culture (the first callus could be detected after 6–8 weeks). Then, calli were collected and transferred into a 500 mL Erlenmeyer flask with 25 mL suspension-medium with 1 mg L^{-1} NOA to final pH of 5.8. Two weeks later, the calli were transferred into new medium (the same composition as above), but with 150 mL volume of medium. This was repeated, until a homogenous suspension was obtained after 6 weeks.

Genotyping

The putatively transformed *V. rupestris* cells were spun down (4000 rpm, 10 min) in a 25-mL Falcon tube, and genomic DNA was extracted using a cetyl trimethyl ammonium bromide (CTAB) based protocol (Doyle and Doyle, 1987). The purified DNA was then probed for presence of the Arabidopsis *TUB6* gene (Arabidopsis *β-tubulin 6* (At5g12250)) using the primers 5′-CGATGTTGTACGCAAAGAGGCTG-3′ and 5′-GACGAGGGAAAGGAATGAGGTTC-3′, yielding a PCR product with an expected size of 436 bp, and using 30 cycles of 10 s denaturation, 10 s annealing at 63 °C, and 50 s extension.

Phenotyping cellular responses and treatments

PCV as indicator for growth, mitotic index, and viability were measured as described by Guan et al. (2013a). Based on our previous work (Guan et al., 2013a), flg22 and Harpin Z (HrpZ) were chosen as elicitors to trigger either basal innate immunity (PTI (pathogen-associated molecular pattern (PAMP) triggered immunity), flg22), or cell-death related effector-triggered immunity (ETI)-like responses (HrpZ). Aliquots of 20 μL from the suspension were placed on a slide and covered with a coverslip for microscopy after 3 days of cocultivation with 100 nM flg22 (as mock control, water was used), 1.7 μM HrpZ (as mock control, 5 mM MES were used), or with 500 μM (±)-jasmonic acid (JA) (Sigma–Aldrich, Germany) (100 mM of a stock solution in absolute ethanol were diluted with distilled water as mock control, water was used). For short-term experiments, 10 μM flg22, 15 μM HrpZ and 500 μM JA were diluted to the final concentration by thoroughly, but gently mixing 50 μL of a suspension (collected at day 3 after subcultivation) in an 1.5-mL reaction tube. Again, an aliquot of 20 μL was placed directly on a slide for microscopy. The time interval between addition of the agent until recording of the first image was less than 2 min, the overall time duration under microscopy never exceeded 20 min. In experiments on auxin-dependent reversion of MTs responses triggered by HrpZ or JA, 10 μM indolyl-3-acetic acid (IAA) were added 20 min after treatments with either 15 μM HrpZ or 500 μM JA (mixed in a 1.5-mL reaction tube). For dose–response studies of MT responses to auxin, different concentrations of IAA were added at subcultivation and assessed at day 3. Salinity stress was administered by incubation in 79 mM NaCl (as mock control, water was used), osmotic stress by 25% PEG 6000 (as mock control, water was used). Cells were examined by microscopy 3 days after the onset of stress treatments.

Microscopy

Making use of the GFP-*At*TUB6 marker, MT responses to the different treatments described above were followed over time in individual cells by spinning disk confocal microscopy, time-lapse series were recorded by capturing z-stacks every 2 min over a period of at least 20 min.

Confocal z-stacks were recorded with an AxioObserver.Z1 (Zeiss, Jena, Germany) using a glycerine immersion 63× LCI-NeofluarImmCorr DIC objective (NA 1.3), the 488-nm emission line of an Ar–Kr laser, and a spinning disk device (Yokogawa CSU-X1 5000).

Quantitative image analysis of microtubules

The method by Higaki et al. (2010) was used to quantify the degree of MT bundling and density: in brief, the original z-stacks were processed by skeletonization using macros integrated in the quantitative image processing software ImageJ (For details see http://hasezawa.ib.k.u-tokyo.ac.jp/zp/Kbi/HigStomata) as shown in Suppl. Fig. 1. The skewness of the intensity distribution over cytoskeletal pixels (reporting the degree of microtubular bundling) was used for quantification (Higaki et al., 2010): these values increase when the incidence of highly fluorescent pixels increases in consequence of MT bundling:

$$\text{skewness} = \frac{1}{N}\sum_{i=1}^{N}\left(\frac{i_n - \bar{i}}{\sigma}\right)^3$$

$$\sigma = \frac{1}{N}\sum_{i=1}^{N}(i_n - \bar{i})^2$$

with N total number of cytoskeletal pixels, i_n intensity of a given pixel, and $\bar{i}$ mean pixel intensity.

Results

Generation of V. rupestris calli and suspension cells expressing GFP-AtTUB6

A fluorescently tagged MT marker cell line was generated from a suspension line of the wild North American grapevine species *V. rupestris* (Qiao et al., 2010) using *Agrobacterium*-mediated stable transformation. Green fluorescent calli (Fig. 1A and B) with cells that showed MT-like filamentous structures (Fig. 1C, cell c and D) were first examined 4 weeks after transformation, and then subcultured every 4 weeks, till enough callus had accumulated over 3 months to generate a suspension cell line. Already in the callus stage, clear cortical MTs were visible (Fig. 1C cell c and D). In contrast, cells that did not express the marker and therefore were seriously affected by the selection, only showed a faint unstructured autofluorescence (Fig. 1C cells a, b and D). After transition to suspension growth, all cells of the stably transformed cell line exhibited clear cortical and radial arrays of MTs (Fig. 1E). The transgenic line was phenotyped with respect to growth, mitotic index, mortality and differentiation over the cell cycle and no differences from the non-transformed wild type could be detected (data not shown).

To verify the correct insertion of the transgene, the transgenic cells were genotyped by genomic PCR probing for the presence of the Arabidopsis *TUB6* gene (Arabidopsis *β-tubulin 6* (At5g12250)) (Suppl. Fig. 2). As expected, only PCR with genomic DNA as template, extracted from the transformed cells, but not from the non-transformed control yielded a band of the predicted size (436 bp).

By constructing optical z-stacks using spinning-disk microscopy, the details of the three-dimensional organization of MTs could be followed (Fig. 2): In addition to cortical MTs that form parallel, transverse, arrays in cells undergoing elongation,

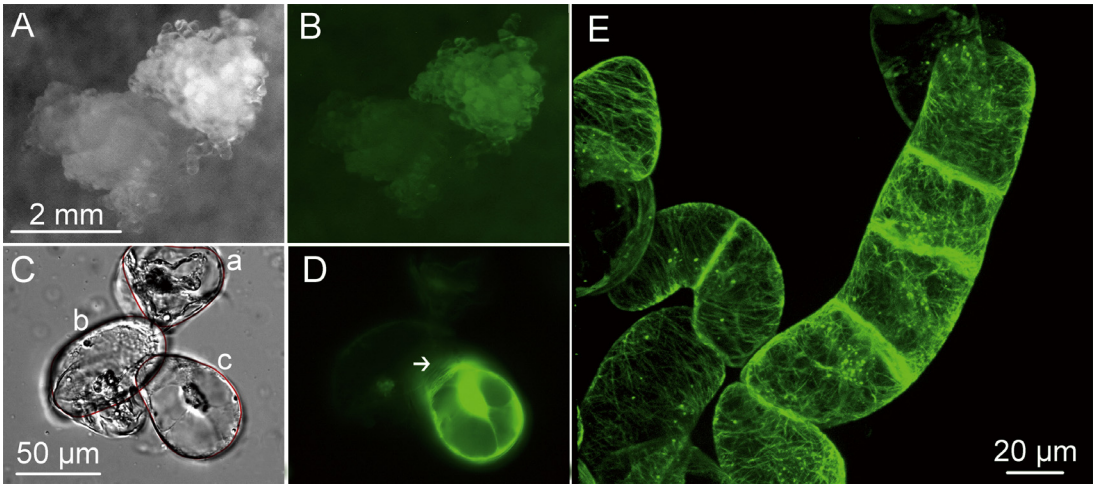

Fig. 1. Generation of a transgenic *V. rupestris* cell line and suspension cells (C: dic; D: GFP filterset) expressing *GFP-AtTUB6*. Primary calli 4 weeks after transformation under the fluorescence stereo microscope (A: bright field, B: GFP filterset) and visualized by spinning-disk confocal microscopy (C: differential interference contrast, D: GFP signal). A successfully transformed cell (a) is shown in comparison with two non-transformed companions (b and c). White arrow in D indicates cortical MTs. (E) Fluorescently tagged arrays of interphase microtubules in the cell line *V. rupestris* GFP-AtTUB6 cultivated in suspension.

and transvacuolar MTs emanating from the nucleus, a part of the tubulin was present in form of fluorescent speckles. These speckles were occasionally seen also in the central (Fig. 2E) and cortical (Fig. 2F) regions, but in most cases they were associated with the nucleus (Fig. 2A–C).

Monitoring the morphogenetic response to defense-related and abiotic stresses

The effect of defense-related stresses, mimicked by flg22 (pathogen-associated molecular pattern (PAMP) triggered immunity, PTI), HrpZ (effector-triggered immunity (ETI)), and JA (wounding), as well as three abiotic stresses represented by sodium chloride (salinity stress), polyethylene glycol 6000 (osmotic stress), and 4 °C (cold) were monitored with respect to culture growth (difference in packed cell volume, PCV), and mortality three days after the onset of stress treatment (Suppl. Fig. 3). The concentrations and incubation time had been derived from previous studies in the non-transformed cell line (Guan et al., 2013a; Ismail et al., 2012; Hamayun et al., 2010). All treatments affected cell growth as reflected by a reduced increase of PCV. For salt stress (79 mM NaCl), osmotic stress (25% PEG 6000), and 1.7 µM HrpZ, this inhibition was extreme and linked with a high rate of cell death. In contrast, treatment with flg22 reduced growth only slightly (to 86% compared to control). Interestingly, JA and cold stress inhibited growth, while mortality was low, indicating that these cells remained viable, but were arrested either in division or expansion.

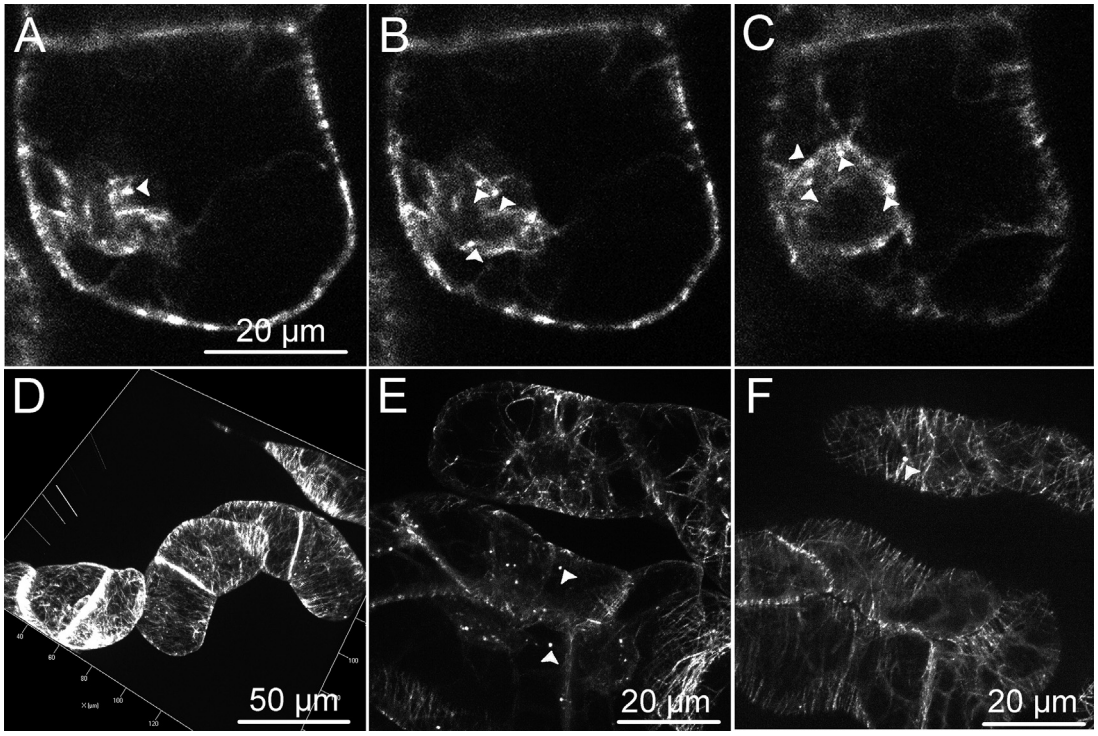

Fig. 2. Confocal sections from a z-stack and geometrical projection of the stack for *V. rupestris* suspension cells expressing *GFP-AtTUB6* to show the spatial organization of MTs. (A–C) Individual sections in *z*-intervals of 1.5 µm. White arrowheads in indicate fluorescent tubulin speckles associated with the nucleus. (D) Geometrical projection of a z-stack. (E and F) Cells with speckles out of the nuclear regions: in transvacuolar strands (E), and the cortical layer (F) of the same cells (indicated by arrowheads).

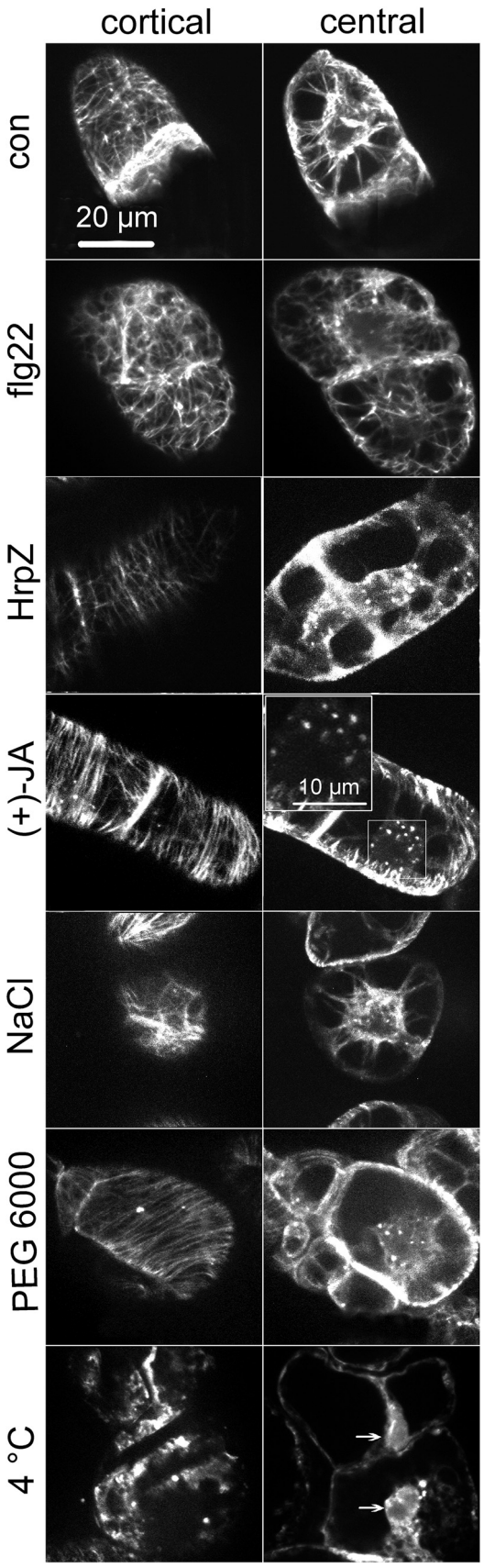

Fig. 3. Sustained responses of microtubules *in vivo* in *V. rupestris* cells expressing the *GFP-AtTUB6* marker after 3 d of treatment with defense-related (flg22, HrpZ, JA), and abiotic (NaCl, PEG 6000, cold-treatment) stress visualized by spinning-disk confocal microscopy. Cells imaged in the cortical and central regions of the cell are shown for control conditions (con), and after the challenge with 100 nM flg22, 1.7 μM HrpZ, 500 μM JA, 79 mM NaCl, 25% PEG 6000, or 4 °C, respectively. White bordered arrows in the 4 °C experiment indicate intranuclear tubulin speckles observed in the cell center region. Representative images from at least five independent experimental series with a population of 100 individual cells for each treatment are shown.

Sustained microtubule response to defense-related and abiotic stresses

In the next step, we verified whether the visualized MTs preserve responsiveness to stress-related stimuli at day 3 after challenge. The PAMP flg22 (100 nM) disordered both radial MTs emanating from the nucleus and the cortical MTs underneath the membrane. Moreover, radial MTs appeared thinner and less, and cortical MTs were somewhat disordered as compared to the control and increased in number (Fig. 3). In contrast, treatment with 1.7 μM HrpZ eliminated the radial MTs, whereas cortical MTs compared to the control appeared more numerous and thinner and aligned in parallel (Fig. 3). These observations are consistent with those made for the same marker in the background of tobacco BY-2 cells (Guan et al., 2013a). In response to 500 μM JA (since JA is not very stable, the effective concentration is perhaps much lower) cortical MTs were organized into bundled, parallel arrays, whereas radial MTs were eliminated. Treatment with 79 mM NaCl caused strong bundling and disorientation of both cortical and radial MTs. Moreover, the cortical MTs appeared disoriented. Bundling of cortical MTs was also observed following treatment with 25% PEG 6000, but here, the parallel orientation of cortical MTs was maintained. Instead, the radial MTs had disappeared. Interestingly, for all of these three conditions, intranuclear speckles of fluorescence were conspicuous (indicated by the white square in the JA experiment). When cells were exposed to 4 °C, both cortical and radial MTs were absent, but again, fluorescent speckles were seen in the nucleus (Fig. 3, arrows). These speckles were observed inside of the nuclear envelope in individual confocal sections and therefore appear to be localized in the karyoplasm. These experiments were accompanied by appropriate controls, where neither cortical nor radial MTs were eliminated nor bundled.

Rapid microtubule responses to HrpZ and JA

Since MT organization depends on the developmental state of a cell and since cells in a suspension differ with respect to this state (although the cells as a population proceed through an ordered sequence of proliferation, expansion, and individualization), it is difficult to infer the more subtle responses relevant for sensing from a statistical snapshot over the population. We therefore followed time-series for individual cells that were mounted on slides and challenged directly under the microscope with the respective stress factor (HrpZ and JA). In parallel, time series were conducted for mock controls to account for effects of the experimental set-up and possible effects of bleaching due to microscopic excitation. We used a relatively mild treatment of HrpZ (15 μM for 45 min). This concentration was chosen based on our previous results in BY-2 (Guan et al., 2013a), where 57.6 μM were suited to trigger a rapid response and taking into account that the sensitivity of *V. rupestris* is ~2.5-fold higher than that of BY-2 as monitored by apoplastic alkalinization. This HrpZ treatment affected MTs in three ways: (i) the radial array became bundled and reduced in number, which was detectable already from 5 min (Fig. 4A) and conspicuous from 10 min after an addition of HrpZ. From 20 min, a few intranuclear speckles were observed. (ii) The cortical array progressively lost its parallel orientation at a similar time scale as the bundling of radial MTs. During the first 5 min of incubation with HrpZ, the number of cortical MTs decreased transiently, followed by as subsequent increase of disoriented MTs. (iii) Cortical MTs became thinner, but

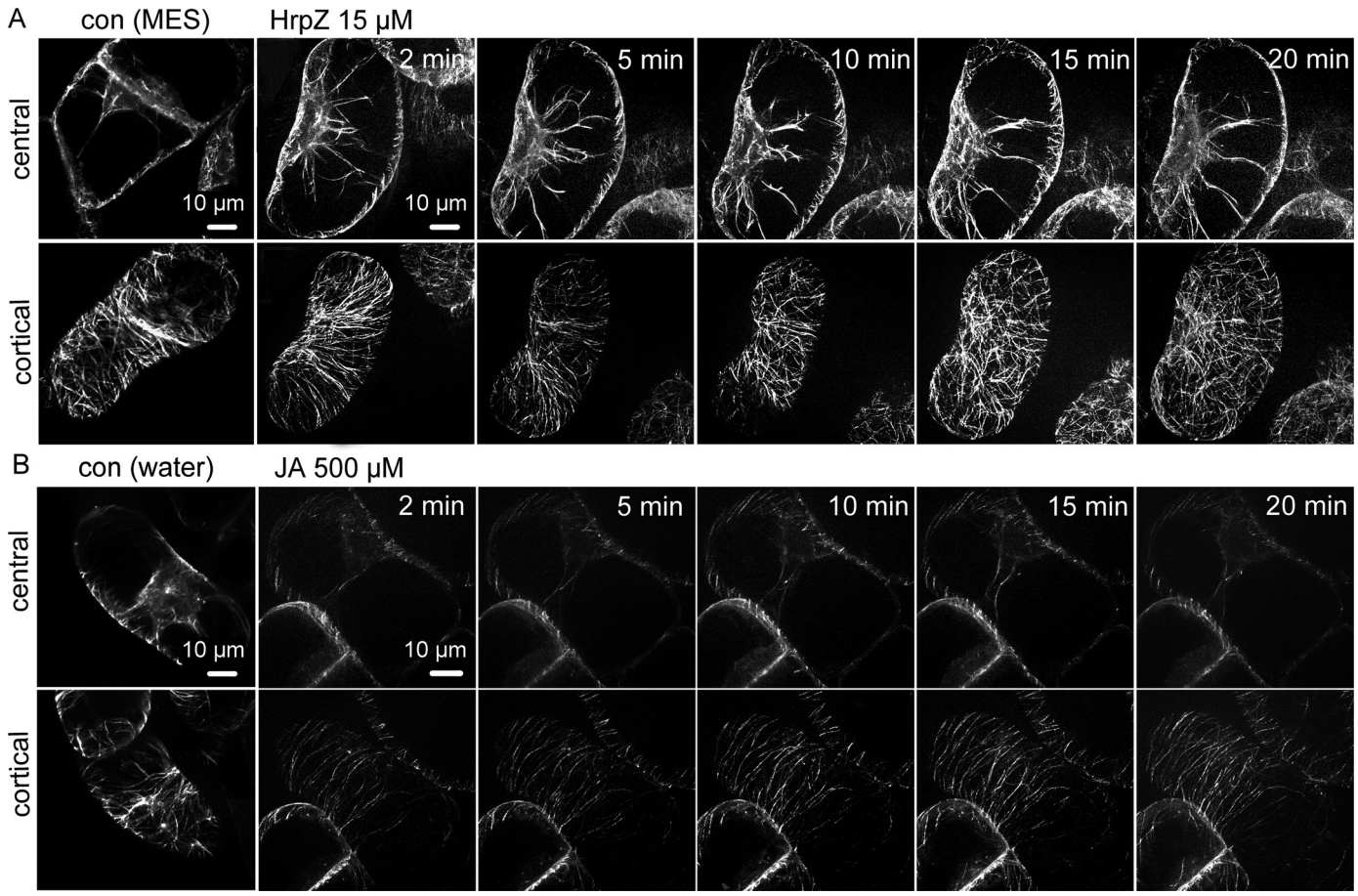

Fig. 4. Immediate response of microtubules to HrpZ and JA. In *V. rupestris* visualized by the GFP-*At*TUB6 marker and spinning-disk confocal microscopy. Confocal sections of time-lapse series collected in the cell center and the cortical regions of the same cell are shown. Controls show the response to the solvent (5 mM MES buffer). (A) Microtubular response to 15 μM HrpZ over the first 20 min and (B) microtubular response to 500 μM JA over 20 min. Controls show the response to water as mock control.

this was evident only from 20 min after addition of HrpZ. A quantitation of this effect by measuring the skewness of cortical MTs showed a reduction by around 50% compared to the control value at 20 min (Fig. 5A).

To observe the response to JA within the limited time frame of observation on a microscopy slide, it was necessary to increase the concentration of the hormone beyond the around 50 μM often used for sustained treatments. Since JA is volatile and only poorly membrane-permeable, the effective concentration of JA is much lower than the nominal value. To obtain a clear response 500 μM JA was used. A treatment with JA caused a rapid increase in the number of cortical MTs accompanied by bundling (Fig. 4B). Both effects were already detected at the earliest observable time point (2 min). When the dose of JA was lower, e.g. 50 μM in the range of normal physiological condition, it takes too long for cells maintaining on slide; whereas increased beyond the 500 μM used in this experiment, both phenomena were accelerated to such a degree that the response could not be followed due to limitations in the handling of the sample. When JA-induced bundling was quantified by measuring the skewness of cortical MTs (Fig. 5B), values of around 3-fold as compared to the controls were seen already at 2 min after addition of JA; these values slowly dropped during the subsequent 20 min to around 2.5-fold.

Auxin can modulate the microtubule response to JA

Stress responses require that resources used for growth be allocated to defense or adaptation. Auxin as most important activator of growth is thus a primary switch for this allocation. We therefore investigated the influence of different concentrations of the natural auxin (indolyl-3-acetic acid (IAA)). To relate the MT response to the physiological context, PCV and mitotic index were determined in parallel (Suppl. Fig. 4). Mitotic index appeared slightly elevated from 10 μM IAA, but this stimulation was not statistically significant. In contrast, PCV was slightly but significantly induced at 10 μM IAA, and then conspicuously suppressed at 100 μM IAA. Given the fact that mitotic activity was not impaired by 100 μM IAA, this is evidence for a strong inhibition of cell expansion. Thus, the dependency of cell expansion on auxin follows the classical bell-shaped dose relation. The steady-state response of MTs to auxin (assessed at day 3 after addition of IAA) followed a similar pattern: cortical MTs were thinner after treatment with low and medium concentrations of IAA, whereas they again were thicker for 100 μM, i.e. this concentration that was superoptimal with respect to cell expansion (Fig. 6A). This impression was supported by quantification of MT thickness. The skewness values were significantly reduced (by around 30%) already at 0.1 μM of IAA and remained low for 1 and 10 μM of IAA. For a high concentration of 100 μM concentrations, the skewness value returned to the value observed for cultivation without IAA.

Interestingly, the thinning of cortical MTs was accompanied by a concomitant response for the incidence of tubulin speckles (Fig. 6B). Although some of them were perinuclear, some were observed clearly inside the nuclear rim (Fig. 6B, inset and zoom-in for 10 μM IAA). Since these images represented *single confocal sections*, these speckles were likely to be located in the karyoplasm. In control cells around 15% of nuclei were free of speckles, this frequency increased to 35% in presence of 10 μM IAA, but dropped back to the

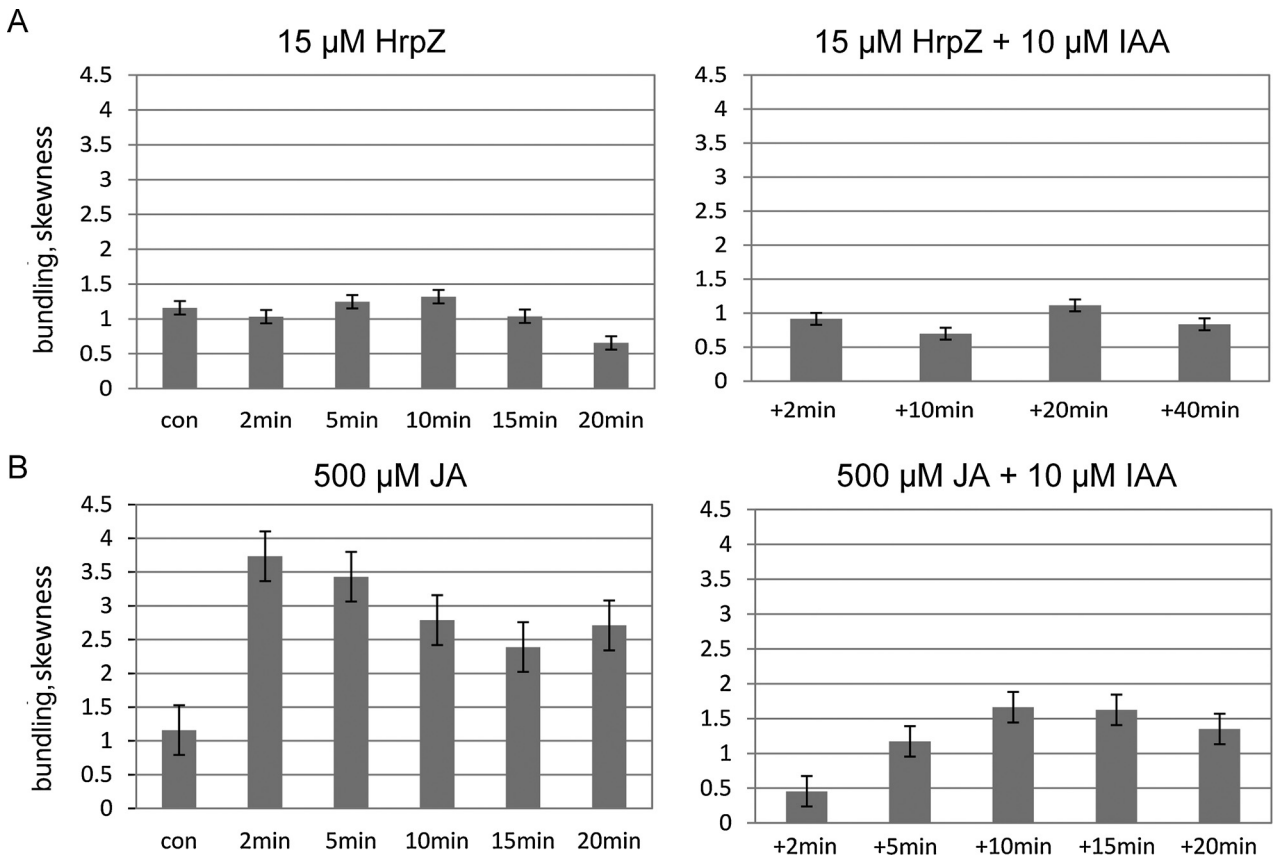

Fig. 5. Response of microtubule bundling to HrpZ and JA and subsequent addition of IAA as quantified by quantitative image analysis based on skewness values of cortical microtubule. Time course of skewness value in response to 15 µM HrpZ (A left) and 500 µM JA (B left). After 20 min, 10 µM of IAA were added and skewness value followed for additional 40 min (HrpZ, A right), or 20 min (JA, B right). Values represent mean and standard errors from at least five independent experimental repeats.

control value, when the concentration of IAA was raised to 100 µM. Thus, there is an inverse relationship between the appearance of intranuclear speckles and the thickness of cortical MTs.

Since incubation with 10 µM IAA reduced MT thickness, we asked whether this treatment can revert the responses to HrpZ and JA. The skewness value as measure for the thickness of cortical MTs was followed over time (Fig. 5B). For HrpZ, the somewhat reduced skewness value of around 0.5 at 20 min after addition of HrpZ had returned to almost the control level already 2 min after addition of IAA and remained more or less at this value during the subsequent 40 min. However, since the response of the skewness value to HrpZ was relatively weak, the amplitude of this reversion was small as well. It should be noted, however, that skewness value was increased (and not decreased) by the auxin treatment. For JA, the response was qualitatively different. Here, the 2.5-fold increased skewness value 20 min after the addition of JA had dropped to less than a fifth of this value already 2 min after addition of IAA, but eased off back to around the value observed in untreated controls. Thus, the effect of IAA on cortical MTs is qualitatively different between HrpZ and JA: in case of HrpZ, IAA induces a rapid (but small) increase of skewness value, whereas in case of JA, IAA induces a rapid (and substantial) decrease of skewness value.

Discussion

Generation of tubulin marker line V. rupestris expressing GFP-AtTUB6

In addition to their role for cellular architecture, MTs have emerged as important components for signaling hub processing stress signals (for review see Nick, 2013). To address this sensory role of microtubules requires visualization systems that allow to follow MT responses in living cells. For this purpose, we have successfully generated the first MT marker line for grapevine. In this suspension cell line of *V. rupestris*, the GFP signal not only monitors a normal organization of MTs, but the tagged MTs maintain their responsiveness to different stress-related signals. The observed response patterns are consistent with those observed in GFP tagged marker lines of tobacco BY-2 (Schwarzerová et al., 2006; Guan et al., 2013a) or those visualized by immunofluorescence in the non-transformed *V. rupestris* line (Qiao et al., 2010; Chang and Nick, 2012). Fluorescently tagged MT transgenic marker lines have been generated for Arabidopsis (Shaw et al., 2003), and tobacco BY-2 cells (Kumagai et al., 2001; Hohenberger et al., 2011), and have been useful to analyze MT functions in viral infection, plant organ growth polarity, phragmoplast MT array, as well as for resistance to biotic and abiotic stress factors (Ruggenthaler et al., 2009; Buschmann et al., 2009; Murata et al., 2013).

Since a stably transformed MT marker line was now also available for grapevine as a third important plant model, we were now exploiting this tool to follow short-term responses of MTs. To detect the early responses, we used time series of individual cells in combination with quantitative image analysis, and by this strategy we were able to overcome limitations of our previous work, where we had to rely on immunofluorescence to visualize MTs. Since immunofluorescence requires chemical fixation, only bulk changes of cytoskeletal organization could be rendered evident against the background of cellular heterogeneity in the suspension. However, also for the life-cell imaging possible by virtue of the novel marker line, statistical data will be required and that this will need to analyze populations of cells. This is possible on a microscopy slide, by

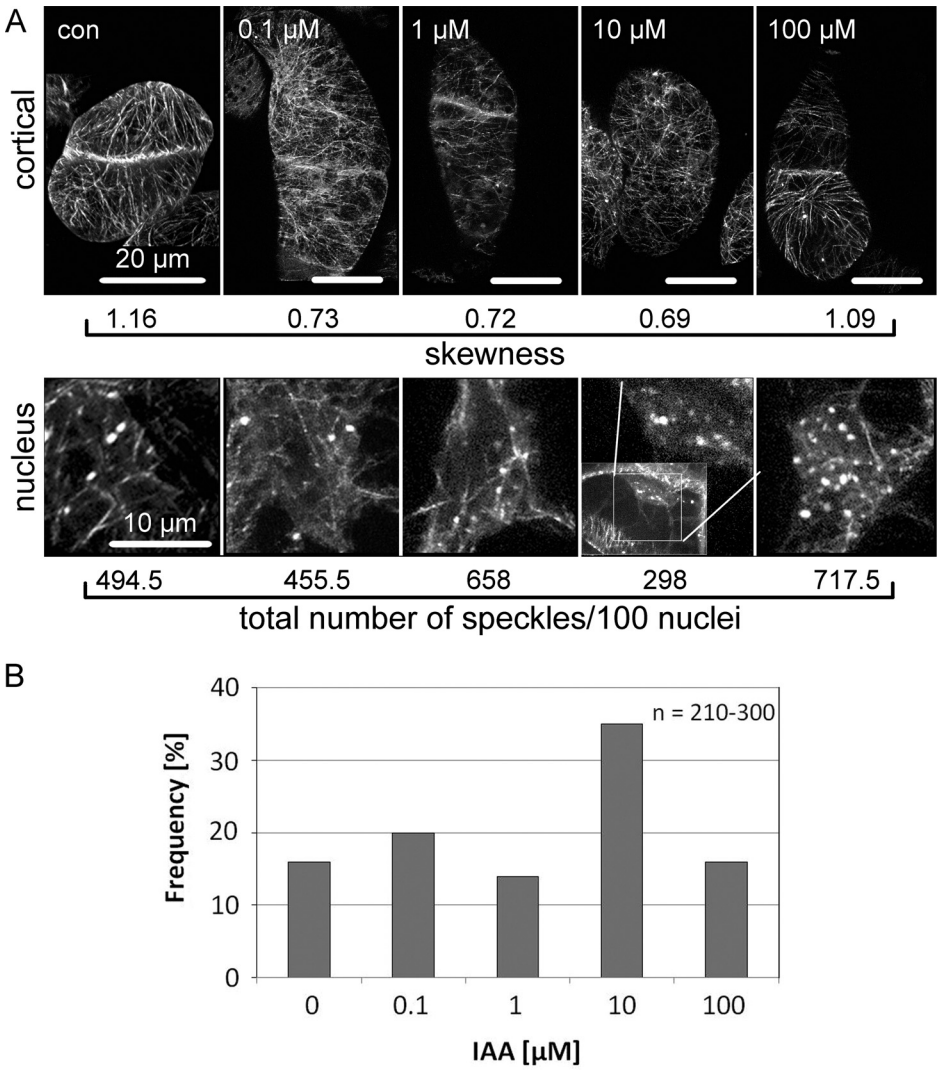

Fig. 6. Sustained microtubular responses over variable dose of exogenous IAA in *V. rupestris* expressing GFP-*At*TUB6. Representative images were collected and quantified after 3 days of auxin treatment. (A) Response of MTs in *V. rupestris* cells to IAA *in vivo* visualized by the GFP-*At*TUB6 marker and spinning-disk confocal microscopy. Geometric projections from z-stacks collected in the cortical or the nucleus region of the cells are shown. Quantitative data for skewness (upper row) and total number of speckles per 100 nuclei (lower row) are added below the images. Insert image in 10 μM IAA nucleus panel indicates the presented region in a cell. (B) Relative incidence of nuclei without speckles after incubation with different IAA concentrations. Quantitative data represent populations of 210–300 individual cells from at least three independent biological replicates for each treatment.

combining random sampling (for instance using algorithms such as the Zeiss MosaiX function) with quantitative image analysis. This will lead to a systematic underestimation of microtubular responsiveness and was recognized as a serious constraint in our previous work with grapevine cells (Qiao et al., 2010; Chang and Nick, 2012). We used HrpZ, a trigger that can induce in *V. rupestris* an ETI-like cell-death response (Chang and Nick, 2012), and JA, a signal that conveys a general response to abiotic stress including salinity stress (Ismail et al., 2014a) to search for rapid MT responses. In fact, we were able to observe, for both triggers, rapid and specific responses of MTs that proceed within a few minutes and thus fall into the earliest observable stress responses observed in *V. rupestris* cells along with apoplastic alkalinization or generation of reactive oxygen species (Qiao et al., 2010; Chang et al., 2011; Chang and Nick, 2012; Ismail et al., 2012).

The expression of the tubulin marker was driven by the strong cauliflower mosaic virus 35S promotor. Overexpression of tubulin has been found to be problematic in many organisms (for review see Breviario and Nick, 2000) and this leads to the question why stable transformation of this marker into the *V. rupestris* line yielded a strain with normal morphology, proliferation, growth and development. The most likely reason for the negative impact of tubulin overexpression is that an excess of soluble tubulin dimers will prevent the self-organization of microtubule arrays and thus impair tubulin functionality. However, in contrast to transformation into plants, transformation of cell suspensions will result in a population of transgenics, where the transgene has been inserted into different sites of the genome in individual cells. Due to the above-mentioned problems caused by excessive tubulin, the lines with very high overexpression will be selected out. By virtue of the antibiotic selection during recovery, we can, on the other hand, eliminate those cells, where the expression of the transgene is very low and therefore end up with a population of transgenic cells, where the expression is moderate and does not interfere too much with the physiology of the cell.

Microtubule responses to HrpZ and JA

For HrpZ, radial MTs became progressively bundled. This was followed by a slower deterioration of the cortical array with first

disordered and subsequently thinner MT bundles. This observation would be consistent with a model, where either activity or abundance of MT-associated proteins is repartitioned into the transvacuolar strands and where MTs, due to competition for free tubulin heterodimers are progressively depleted from the cortex and renucleated around the nucleus. This repartitioning might be linked with the contraction of actin towards the nucleus (Guan et al., 2013a) as earliest manifestation of ensuing programmed cell death (for review see Smertenko and Franklin-Tong, 2011). Radial microtubule arrays have been proposed to be organized by dynein motors in animal cells. For instance, it has been known in melanophores that dynein induces nucleation-dependent formation of MT radial array (Vorobjev et al., 2001; Malikov et al., 2004). So far, despite intensive searches, no dyneins could be detected in any higher plant genomes. The mechanisms for organizing the radial array of MTs during dyneins-dependent activities must be different in plant from animal/fungi. Since many proteins are evolutionarily conserved among eukaryotes, it holds true in proteins particularly involved in intracellular motility. For instance the formation of spindle poles, in animals and fungi dynein are required to organize; while plant develops specific mechanisms in interphase and during mitosis without dynein (for review see, Nick, 2013; Merdes et al., 2000; Lawrence et al., 2001). One report for a *in-silico* detection of a dynein-like protein in rice, was later retracted as sequencing artefact (King, 2002). However, a plant specific actin-microtubule cross-linking kinesin, KCH that can dynamically shuffle between cortex and perinuclear cytoplasm would be molecular candidates for this function (Klotz and Nick, 2012).

For JA, the situation is qualitatively different: here, cortical MTs are rapidly bundled and increase also in number, which would be consistent with activation (or *de-novo* synthesis, or allocation) of MT-associated proteins in the cell cortex. These bundles of MTs might be linked to the so called macrotubules reported as early markers of the response to osmotic stress (Komis et al., 2002). Such macrotubules have been known for a long time from *in vitro* studies (Warfield and Bouck, 1974) and consist of tightly coiled helices formed by longitudinal compaction of loosely coiled protofilament pair intermediates. In extreme cases, MTs can even form highly organized paracrystals (Marantz and Shelanski, 1970) and bifilar helices (Hinkley, 1978). These macrotubules are not a mere byproduct of the osmotic stress response, but actually were shown to be necessary for osmoadaptation (Komis et al., 2002). Although the molecular details of macrotubule formation are to be elucidated, it is thought to require a partial deconstruction of the cortical array followed by *de-novo* nucleation (Komis et al., 2002). It should be noted that also in our system MTs responses were different induced by salinity stress and by osmotic stress imposed by polyethylene glycol (Fig. 3). Both salinity and drought cause osmotic stress. However, salinity not only imposes osmotic stress, but in addition ionic stress from uptake of sodium ions through nonselective cation channels (for review see Ismail et al., 2014b). The disordering of cortical MTs in response to salt stress, might be linked with the salinity triggered detachment of the MT-associated protein SPIRAL1 (Wang et al., 2011). The salt induced bundling of MT is accompanied by a depletion of finer MTs and an increase of diffuse cytoplasmic fluorescence probably representing disassembled tubulin heterodimers (Suppl. Fig. 5C). Also the response to JA is rapid as presented in Suppl. Fig. 5B and involves an increase in MT bundling. Salt stress had been shown in the same cell line to stimulate JA synthesis (Ismail et al., 2014a) and signaling (Ismail et al., 2012). A straightforward mechanism would be that the activation of the JA-pathway by osmotic stress is responsible for the formation of macrotubules. This could be tested by inhibitors of JA synthesis such as phenidone or antagonists of JA signaling such as salicylic acid that have been shown to impair salinity adaptation in grapevine cells (Ismail et al., 2012).

Stress responses are in many cases accompanied by a rapid inhibition of growth. The evolutionary background for this phenomenon is to allocate resources otherwise used for expansion for stress adaptation (for a critical review on this growth differentiation balance and concurrent theories see Stamp, 2003). As to be expected, a knock-down of defense related traits has been shown to result in higher growth rates (Züst et al., 2011). Cortical MTs are central regulators of expansion growth and this MT function is controlled by auxin (recently reviewed in Nick, 2012). We therefore asked, whether and how auxin alters MTs in *V. rupestris*, and whether exogenous auxin might modulate the microtubular response to stress signals (represented by HrpZ and JA, respectively).

Exogenous auxin alters microtubules to stress signals HrpZ and JA

We observed that the thickness of cortical MTs was modulated by auxin and that this auxin response followed a characteristic bell-shaped curve where MTs became thinner at concentrations up to 10 μM. Since the dose–response of cell growth of auxin follows a bell-shaped curve and since this bell-shaped relation had also been demonstrated for auxin-dependent microtubule orientation (Nick et al., 1992), we also probed for the effect of very high auxin concentrations (up to 100 μM) that were superoptimal for cell expansion. In fact, we were able to show that MTs returned to their original thickness, confirming that also this auxin-dependent phenomenon followed a bell-shaped response relation. The thickening of MTs induced by JA could be reverted by supplementary auxin. This reversion occurred within extremely short time (less than 2 min) and was thus much faster than the preceding JA-induced thickening indicating a mechanism, where bundles of MTs split into finer fibers by removal of cross-linking proteins rather than by disassembly and reassembly. For HrpZ, both the microtubular effect to the stress agent as well as the influence of exogenous auxin were qualitatively different. HrpZ induced a slow depletion of the cortical array (preceded and possibly caused by a preceding bundling of perinuclear MTs), and auxin partially reverted this phenomenon, again within a few minutes, again pointing to a modulation in the activity of MT cross-linking proteins. The sign-reversal in the microtubular response to auxin (dissociation of cortical MT bundles after pretreatment with JA, stimulation of cortical bundling after pretreatment with HrpZ) means that the cellular competence to the auxin signal is not constant, but modulated by cross-talk with other signals, e.g. PIN proteins. In Arabidopsis, accumulating evidence directed to the relation of cortical MT orientation and the cellular localization of PIN proteins and thus polar auxin transport. The MT orientation regulators CLASP and MAP65 control the abundance of polarity regulator PINOID kinase at the plasma membrane (Kakar et al., 2013). Cortical MTs can mediate petiole elongation during shade avoidance by regulating the expression of cell wall modifying proteins XTHs via control of auxin distribution (Sasidharan et al., 2014). Moreover, the polarity of auxin transport is linked to the cycling of pin-formed protein related to actomyosin-dependent vesicle traffic (Maisch and Nick, 2007). The continuously cycling of auxin between plasma membrane and intracellular compartments has been proposed to depend on actin filaments (Nick, 2010). Such a modulation of auxin-responsiveness by JA had been demonstrated previously in the context of gravitropic curvature in rice (Gutjahr et al., 2005). Whether HrpZ can alter auxin responsiveness as well, remains to be elucidated.

Intranuclear tubulin and the prevention of tubulin toxicity

During the present work, intranuclear fluorescent speckles were observed in the karyoplasm of cells challenged by various stress factors. Such speckles have been described previously after

cold-induced disassembly of tubulin in tobacco BY-2 cells (Schwarzerová et al., 2006). When these nuclei were purified and probed by protein blotting, they were confirmed to contain tubulin leading to the discovery that plant tubulins harbor nuclear exclusion sequences. Moreover, such intranuclear tubulin is rich in tyrosinated α-tubulin indicating that it does not originate from stable microtubules, but might represent sites of nucleation, supported by previous reports from *Vicia faba* that γ-tubulin enters the nucleus already prior to mitosis, during the G2 phase (Binarová et al., 2000). These findings were later confirmed for animal cells (Akoumianaki et al., 2009). The observation that such speckles are observed not only after cold treatment, but also in response to other stress factors indicates that these speckles are formed following growth arrest. To test this idea, the incidence of such speckles was scored over variable doses of exogenous auxin. In fact, the dose–response pattern shows that the frequency of intranuclear speckles was inversely related with the intensity of auxin-dependent cell expansion (quantification indicated in Fig. 6A), and with the skewness value for cortical MTs. Intranuclear speckles were scarcest, when the cells were exposed to the concentration of IAA optimal for cell expansion. The biological function of intranuclear tubulin is far from understood. However, since nuclear exclusion sequences are found in both animal and plant tubulins, and since intranuclear tubulin has been reported for mammalian cells as well (Akoumianaki et al., 2009), the sequestration of tubulin in the karyoplasm might be evolutionarily conserved. The stress-induced remodeling of MTs should lead to a rapid accumulation of tubulin heterodimers. Similar to other organisms, plants have evolved a couple of mechanisms to circumvent the accumulation of non-assembled tubulin in the cytoplasm. Such tubulin speckles have been observed previously under conditions, where soluble heterodimers form in excess in consequence of bulk disassembly (Ahad et al., 2003; Schwarzerová et al., 2006). Since they are reversible, they are unlikely to represent agglomeration of degrading protein, but seem to be recruited by specific tubulin-binding proteins. For intranuclear speckles that had been shown (Schwarzerová et al., 2006) rich in tyrosinated tubulin indicating that these speckles are not the remaining stubs of stable microtubules, but represent a pool of dynamic microtubules. Elevated levels of free tubulin heterodimers seem to be toxic for most organisms (for review see Breviario and Nick, 2000), and to sequester this free tubulin into the nucleus would be an efficient way to prevent tubulin toxicity.

Future perspective

Cortical MTs seem to interact with other signaling proteins such as phospholipase D to generate a sensory hub that can process stress signals (Dhonukshe et al., 2003; for review, see Nick, 2013). The integration of a GFP-tubulin marker into a cell line that is highly responsive to different stresses and capable to respond to different stress qualities by specific outputs (Qiao et al., 2010; Chang et al., 2011; Chang and Nick, 2012; Ismail et al., 2012) will allow to test the model, whether sensory MTs can decode stress signatures and thus allow the cell to discriminate different qualities of stress. For instance, we are currently in the process of completing a detailed study on the role of microtubules on the signaling culminating in low-temperature adaptation making use of this cell line.

Conflict of interests

The authors declare that there is no conflict of interests whatsoever.

Acknowledgements

This work was supported by BACCHUS Interreg IV project, and a fellowship of the Chinese Scholarship Council (CSC) to Xin Guan. We would like to thank Thorsten Manthey (RLP AgroScience/AlPlanta – Institute for Plant Research, Neustadt an der Weinstraße, Germany) for technical support in transformation.

Appendix A. Supplementary data

Supplementary data associated with this article can be found, in the online version, at http://dx.doi.org/10.1016/j.jplph.2014.10.023.

References

Abdrakhamanova A, Wang QY, Khokhlova L, Nick P. Is microtubule assembly a trigger for cold acclimation? Plant Cell Physiol 2003;44:676–80.
Ahad A, Wolf J, Nick P. Activation-tagged tobacco mutants that are tolerant to antimicrotubular herbicides are cross-resistant to chilling stress. Transgenic Res 2003;12:615–20.
Akoumianaki T, Kardassis D, Polioudaki H, Georgatos SD, Theodoropoulos PA. Nucleocytoplasmic shuttling of soluble tubulin in mammalian cells. J Cell Sci 2009;122:1111–20.
Bertani G. Studies on lysogenesis I. The mode of phage liberation by lysogenic *Escherichia coli*. J Bacteriol 1951;62:293–300.
Binarová P, Cenklová V, Hause B, Kubátová E, Lysák M, Doležel J, et al. Nuclear gamma-tubulin during acentriolar plant mitosis. Plant Cell 2000;12:433–40.
Breviario D, Nick P. Plant tubulins: a melting pot for basic questions and promising applications. Transgenic Res 2000;9:383–90.
Buschmann H, Hauptmann M, Niessing D, Lloyd CW, Schäffner AR. Helical growth of the Arabidopsis mutant tortifolia2 does not depend on cell division patterns but involves handed twisting of isolated cells. Plant Cell 2009;21:2090–100.
Chang X, Heene E, Qiao F, Nick P. The phytoalexin resveratrol regulates the initiation of hypersensitive cell death in Vitis cell. PLoS ONE 2011;6:e26405.
Chang X, Nick P. Defence signalling triggered by Flg22 and Harpin is integrated into a different stilbene output in Vitis cells. PLoS ONE 2012;7:e40446.
Chen H, Nelson RS, Sherwood JL. Enhanced recovery of transformants of *Agrobacterium tumefaciens* after freeze–thaw transformation and drug selection. Biotechniques 1994;16:664–70.
De Amicis F, Patti T, Marchetti S. Improvement of the pBI121 plant expression vector by leader replacement with a sequence combining a poly(CAA) and a CT motif. Transgenic Res 2007;16:731–40.
Dhonukshe P, Laxalt AM, Goedhart J, Gadella TWJ, Munnik T, Phospholipase D. Activation correlates with microtubule reorganization in living plant cells. Plant Cell 2003;15:2666–70.
Doyle JJ, Doyle JL. A rapid DNA isolation procedure for small quantities of fresh leaf tissue. Phytochem Bull 1987;19:11–5.
Godbolé R, Michalke W, Nick P, Hertel R. Cytoskeletal drugs and gravity-induced lateral auxin transport in rice coleoptiles. Plant Biol 2000;2:176–80.
Green PB. Mechanism for plant cellular morphogenesis. Science 1962;138:1401–10.
Guan X, Buchholz G, Nick P. The cytoskeleton is disrupted by the bacterial effector HrpZ, but not by the bacterial PAMP flg22, in tobacco BY-2 cells. J Exp Bot 2013a;64:1805–10.
Guan X, Buchholz G, Nick P. Actin marker lines in grapevine reveal a gatekeeper function of guard cells. J Plant Physiol 2014;13:1164–70.
Guan X, Zhao H, Wang Y. Studies on genetic transformation of grape shoot apical meristems by Agrobacterium-mediated transformation. Vitis 2013b;52:185–90.
Gutjahr C, Riemann M, Müller A, Weiler EW, Nick P. Cholodny–Went revisited – a role for jasmonate in gravitropism of rice coleoptiles. Planta 2005;222:575–80.
Hamant O, Heisler MG, Jönsson H, Krupinski P, Uyttewaal M, Bokov P, et al. Developmental patterning by mechanical signals in Arabidopsis. Science 2008;22:1650–60.
Hamayun M, Khan SA, Shinwari ZK, Khan AL, Ahmed N, Lee I. Effect of polyethylene glycol induced drought stress on physio-hormonal attributes of soybean. Pak J Bot 2010;42:977–80.
Hardham AR, Green PB, Lang JM. Reorganization of cortical microtubules and cellulose deposition during leaf formation of *Graptopetalum paraguayense*. Planta 1980;149:181–90.
Higaki T, Kutsuna N, Sano T, Kondo N, Hasezawa S. Quantification and cluster analysis of actin cytoskeletal structures in plant cells: role of actin bundling in stomatal movement during diurnal cycles in Arabidopsis guard cells. Plant J 2010;61:156–60.
Hinkley RE. Macrotubules induced by halothane: in vitro assembly. J Cell Sci 1978;32:99–100.
Hohenberger P, Eing C, Straessner R, Durst S, Frey W, Nick P. Plant actin controls membrane permeability. Biochim Biophys Acta 2011;1808:2304–10.
Ismail A, Riemann M, Nick P. The jasmonate pathway mediates salt tolerance in grapevines. J Exp Bot 2012;63:2127–30.

Ismail A, Seo M, Takebayashi Y, Kamiya Y, Eiche E, Nick P. Salt adaptation requires efficient fine-tuning of jasmonate signaling. Protoplasma 2014a., http://dx.doi.org/10.1007/s00709-013-0591-y.

Ismail A, Takeda S, Nick P. Life and death under salt stress: same players, different timing? J Exp Bot 2014b., http://dx.doi.org/10.1093/jxb/eru159.

Kakar K, Zhang H, Scheres B, Dhonukshe P. CLASP-mediated cortical microtubule organization guides PIN polarization axis. Nature 2013;495:529–30.

King SM. Dyneins motor on in plants. Traffic 2002;3:930–40.

Klotz J, Nick P. A novel actin-microtubule cross-linking kinesin NtKCH, functions in cell expansion and division. New Phytol 2012;193:576–80.

Kobayashi I, Kobayashi Y. Microtubules and pathogen defence. Plant Cell Monogr 2008;143:121–30.

Komis G, Apostolakos P, Galatis B. Hyperosmotic stress induces formation of tubulin macrotubules in root-tip cells of *Triticum turgidum*: their probable involvement in protoplast volume control. Plant Cell Physiol 2002;43:911–20.

Kumagai F, Yoneda A, Tomida T, Sano T, Nagata T, Hasezawa S. Fate of nascent microtubules organized at the M/G(1) interface, as visualized by synchronized tobacco BY-2 cells stably expressing GFP tubulin: time-sequence observations of the reorganization of cortical microtubules in living plant cells. Plant Cell Physiol 2001;42:723–30.

Lawrence CJ, Morris NR, Meagher RB, Dawe RK. Dyneins have run their course in plant lineage. Traffic 2001;2:362–70.

Ledbetter MC, Porter KR. A microtubule in plant cell fine structure. J Cell Biol 1963;12:239–40.

Liu Q, Qiao F, Ismail A, Chang X, Nick P. The plant cytoskeleton controls regulatory volume increase. Biochim Biophys Acta Membr 2013;1828:2111–20.

Luo Z, Chen Z. Improperly terminated, unpolyadenylated mRNA of sense transgenes is targeted by RDR6-mediated RNA silencing in Arabidopsis. Plant Cell 2007;19:943–58.

Maisch J, Nick P. Actin is involved in auxin-dependent patterning. Plant Physiol 2007;143:1695–700.

Malikov V, Kashina A, Rodionov V. Cytoplasmic dynein nucleates microtubules to organize them into radial arrays in vivo. Mol Biol Cell 2004;15:2742–50.

Marantz R, Shelanski ML. Structure of microtubular crystals induced by vinblastine in vitro. J Cell Biol 1970;44:234–40.

Merdes A, Heald R, Samejima K, Earnshaw WC, Cleveland DW. Formation of spindle poles by dynein/dnactin-dependent transport of NuMA. J Cell Biol 2000;149:851–60.

Murashige T, Skoog F. A revised medium for rapid growth and bioassays with tobacco tissue cultures. Plant Physiol 1962;15:473–80.

Murata T, Sano T, Sasabe M, Nonaka S, Higashiyama T, Hasezawa S, et al. Mechanism of microtubule array expansion in the cytokinetic phragmoplast. Nat Commun 2013;4:1967.

Nakamura M, Naoi K, Shoji T, Hashimoto T. Low concentrations of propyzamide and oryzalin alter microtubule dynamics in Arabidopsis epidermal cells. Plant Cell Physiol 2004;45:1330–40.

Nick P, Schäfer E, Furuya M. Auxin redistribution during first positive phototropism in corn coleoptiles – microtubule reorientation and the Cholodny–Went Theory. Plant Physiol 1992;99:1302–10.

Nick P. Signals, motors, morphogenesis – the cytoskeleton in plant development. Plant Biol 1999;1:169–70.

Nick P. Probing the actin–auxin oscillator. Plant Signal Behav 2010;5:94–8.

Nick P. Microtubules and the Tax Payer. Special Issue Applied Plant Cell Biology. Protoplasma 2012;249(Suppl. 2):S81–90.

Nick P. Microtubules, signalling and abiotic stress. Plant J 2013;75:309–10.

Nick P, Schäfer E, Hertel R, Furuya M. On the putative role of microtubules in gravitropism of maize coleoptiles. Plant Cell Physiol 1991;32:873–80.

Nitsch JP, Nitsch C. Haploid plants from pollen grains. Science 1969;163:85–7.

Qiao F, Chang X, Nick P. The cytoskeleton enhances gene expression in the response to the Harpin elicitor in grapevine. J Exp Bot 2010;61:4021–30.

Ruggenthaler P, Fichtenbauer D, Krasensky J, Jonak C, Waigmann E. Microtubule-associated protein AtMPB2C plays a role in organization of cortical microtubules, stomata patterning, and tobamovirus infectivity. Plant Physiol 2009;149:1354–60.

Sasidharan R, Keuskamp DH, Kooke R, Voesenek LACJ, Pierik R. Interactions between auxin microtubules and XTHs mediate green shade-induced petiole elongation in Arabidopsis. PLoS ONE 2014;9:e90587.

Sataric MV, Tuszynski JA. Nonlinear dynamics of microtubules: biophysical implications. J Biol Phys 2005;31:487–90.

Schellenbaum P, Mohler V, Wenzel G, Walter B. Variation in DNA methylation patterns of grapevine somaclones *Vitis vinifera* L.). BMC Plant Biol 2008;8:78–88.

Schwarzerová K, Petrášek J, Panigrahi KCS, Zelenková S, Opatrný Z, Nick P. Intranuclear accumulation of plant tubulin in response to low temperature. Protoplasma 2006;227:185–90.

Seibicke T. [PhD thesis] Untersuchungen zur induzierten Resistenz an Vitis spec [PhD thesis]. University of Freiburg; 2002.

Shaw SL, Kamyar R, Ehrhardt DW. Sustained microtubule treadmilling in Arabidopsis cortical arrays. Science 2003;300:1715–20.

Smertenko A, Franklin-Tong VE. Organisation and regulation of the cytoskeleton in plant programmed cell death. Cell Death Differ 2011;18:1263–70.

Stamp N. Out of the quagmire of plant defense hypotheses. Q Rev Biol 2003;78:23–55.

Takemoto D, Hardham AR. The cytoskeleton as a regulator and target of biotic interactions in plants. Plant Physiol 2004;136:3864–70.

Vorobjev I, Malikov V, Rodionov V. Self-organization of a radial microtubule array by dynein-dependent nucleation of microtubules. Proc Natl Acad Sci U S A 2001;98:10160–70.

Wang S, Kurepa J, Hashimoto T, Smalle JA. Salt stress-induced disassembly of Arabidopsis cortical microtubule arrays involves 26S proteasome-dependent degradation of SPIRAL1. Plant Cell 2011;23:3412–20.

Warfield RK, Bouck GB. Microtubule–macrotubule transitions: intermediates after exposure to the mitotic inhibitor vinblastine. Science 1974;4170:1219–20.

Wei ZM, Laby RJ, Zumoff CH, Bauer DW, He SY, Collmer A, et al. Harpin, elicitor of the hypersensitive response produced by the plant pathogen *Erwinia amylovora*. Science 1992;257:85–8.

Züst T, Joseph B, Shimizu KK, Kliebenstein DJ, Turnbull LA. Using knockout mutants to reveal the growth costs of defensive traits. Proc Roy Soc B 2011;278:2598–600.